CrystEngComm

PAPER

View Article Online
View Journal | View Issue

Cite this: *CrystEngComm*, 2014, **16**, 5110

Multinuclear coordination polymers based on Ag···Ag interaction: syntheses, structures, and luminescence properties†

Hua-Yu Shi, Yun-Bo Dong, Ying-Ying Liu* and Jian-Fang Ma*

Received 30th January 2014,
Accepted 1st April 2014

DOI: 10.1039/c4ce00236a

www.rsc.org/crystengcomm

A series of coordination polymers based on Ag···Ag interactions, namely, $[Ag_2(hpyb)_{0.5}(L1)_{0.5}(NO_3)]·H_2O$ (**1**), $[Ag_4(hpyb)(HL2)(NO_3)_2]·2H_2O$ (**2**), $[Ag_3(hpyb)_{0.5}(L3)(NO_3)]$ (**3**), $[Ag_6(hpyb)(L4)_2(NO_3)]·NO_3·2H_2O$ (**4**), $[Ag_5(hpyb)_{0.5}(L5)_2(NO_3)]·H_2O$ (**5**), $\{Ag_4(hpyb)[L6(CH_3)_2]_2\}$ (**6**), $\{Ag_6(hpyb)(HL7)_2[L7(CH_3)]\}$ (**7**) and $[Ag_3(hpyb)_{0.5}(HL8)]·H_2O$ (**8**) (H_2L1 = *p*-phthalic acid, H_3L2 = 1,2,3-benzenetricarboxylic acid, H_2L3 = *cis*-2-butenedioic acid, H_2L4 = 2,3-pyridinedicarboxylic acid, H_2L5 = *m*-phthalic acid, H_4L6 = 1,2,4,5-benzenetetracarboxylic acid, H_3L7 = 1,2,4-benzenetricarboxylic acid and H_4L8 = 4,4′-oxydiphthalic acid) has been synthesized. For compounds **1**–**4**, the polycarboxylate anions bridge multinuclear Ag(I) units to form 1D chains, respectively. The chains are extended by π–π interactions into a 2D supramolecular layer for compound **3** and 3D supramolecular architectures for compounds **1**, **2** and **4**. Compound **5** displays a 3D (4,8)-connected $(3^4·4^2)(3^4·4^{12}·5^8·6^4)_2$ framework. Compounds **6**–**8** exhibit 2D layers, where the layers of **6** and **8** are further linked by π–π interactions to yield 3D supramolecular architectures. In the solid state, compounds **1**–**8** exhibit strong fluorescence emission bands at room temperature.

Introduction

Recently, the research of silver complexes has been the subject of considerable interest owing to their fascinating structures and photoluminescence properties.[1] In this regard, the silver clusters are one of the most important factors because of their potential applications in the regions of catalysis, pharmacy and luminescence.[2] An insight into the silver cluster comes from the forces associated with Ag···Ag interactions. It is well known that polycarboxylic acids with various spacers can influence the final structures of the silver complexes.[3] Especially, their carboxylate groups usually exhibit the coordination capability to display diverse binding modes with Ag(I) ions, which may create bi-, tri-, or tetra-nuclear Ag(I) clusters.[4] On the other hand, it is known that well designed neutral ligands, such as various binding sites, with appropriate shapes, are key factors for constructing Ag(I)-containing coordination polymers.[5] So far, a number of silver compounds modified by, *e.g.*, pyridine-, imidazole-, triazole- and tetrazole-based ligands have been reported.[6,7] These ligands can provide multiple coordination sites, which result in structural diversities of the compounds.

Based on the aforementioned consideration, we selected a N-donor neutral ligand hexakis[2-(1*H*-pyrazol-3-yl)pyridinylmethyl]benzene (hpyb, Chart 1).[8] As a multidentate ligand, hpyb affords twelve potential coordination sites. Also, its flexible methylenes can twist and rotate freely to conform to the requirements of metal cations.[9] Although some coordination polymers based on the single 3-(2-pyridyl)pyrazole ligand have been reported,[10] the coordination polymer constructed by both hpyb and polycarboxylates has never been systematically studied to the best of our knowledge.[8] In order to investigate the structural varieties of the Ag(I)-containing coordination polymers, we selected a series of polycarboxylate ligands by retaining the N-donor ligand and inorganic salt invariant.

In this work, eight new silver cluster-based complexes, $[Ag_2(hpyb)_{0.5}(L1)_{0.5}(NO_3)]·H_2O$ (**1**), $[Ag_4(hpyb)(HL2)(NO_3)_2]·2H_2O$ (**2**), $[Ag_3(hpyb)_{0.5}(L3)(NO_3)]$ (**3**), $[Ag_6(hpyb)(L4)_2(NO_3)]·NO_3·2H_2O$ (**4**), $[Ag_5(hpyb)_{0.5}(L5)_2(NO_3)]·H_2O$ (**5**), $\{Ag_4(hpyb)[L6(CH_3)_2]_2\}$ (**6**), $\{Ag_6(hpyb)(HL7)_2[L7(CH_3)]\}$ (**7**) and $[Ag_6(hpyb)(HL8)_2]·2H_2O$ (**8**) (H_2L1 = *p*-phthalic acid, H_3L2 = 1,2,3-benzenetricarboxylic, H_2L3 = *cis*-2-butenedioic acid, H_2L4 = 2,3-pyridinedicarboxylic acid, H_2L5 = *m*-phthalic acid, H_4L6 = 1,2,4,5-benzenetetracarboxylic acid, H_3L7 = 1,2,4-benzenetricarboxylic acid and H_4L8 = 4,4′-oxydiphthalic acid, Chart 1) have been prepared. The photoluminescence properties of these complexes at room temperature have been investigated.

Key Lab of Polyoxometalate Science, Department of Chemistry, Northeast Normal University, Changchun 130024, People's Republic of China.
E-mail: liuyy147@nenu.edu.cn, majf247@yahoo.com; Fax: +86 431 85098620

† Electronic supplementary information (ESI) available: Selected bond distances and angles, structure illustrations for compounds 1–8 and the simulated and experimental PXRD patterns. CCDC 984125–984133. For ESI and crystallographic data in CIF or other electronic format see DOI: 10.1039/c4ce00236a

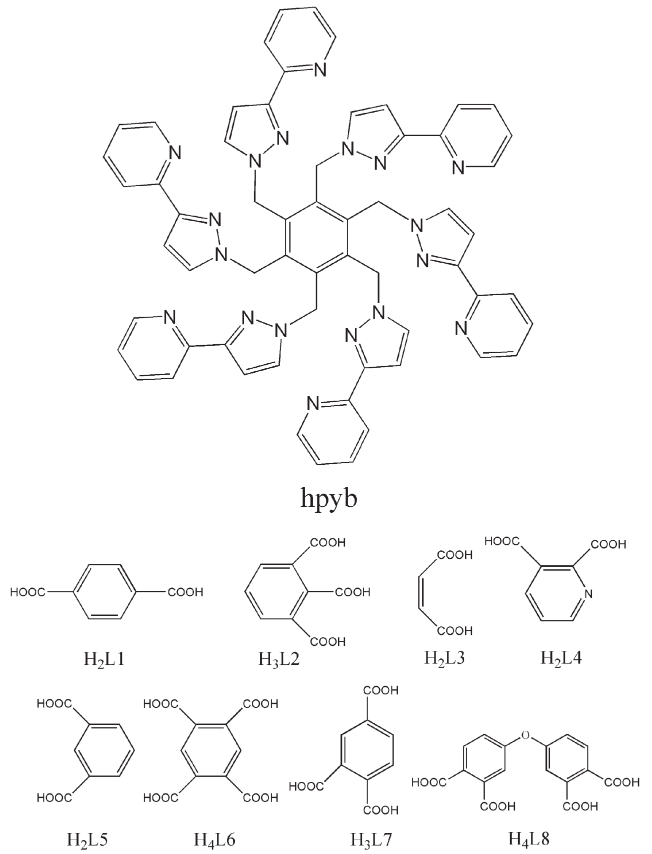

Chart 1 Structures of the hpyb ligand and polycarboxylic acids.

Experimental

Materials and instruments

The 3-(2-pyridyl)pyrazole and hexakis(bromomethyl)benzene were synthesized according to the known method.[11] All other chemicals were commercially available without further purification. Elemental analyses (C, H, N) were performed on a Perkin-Elmer 240 analyzer. Powder X-ray diffraction (PXRD) data were collected by a Rigaku Dmax 2000 X-ray diffractometer. A Mattson Alpha Centauri spectrometer and a Perkin-Elmer FLS-920 spectrometer were used to obtain the FT-IR spectra and fluorescence spectra, respectively. The photoluminescence properties were measured on a FLSP920 Edinburgh fluorescence spectrometer.

Synthesis of hpyb. A mixture of 3-(2-pyridyl)pyrazole (15 mM, 2.18 g), NaOH (15 mM, 0.60 g) and DMSO (40 mL) was stirred at 80 °C for 1 h. Then hexakis(bromomethyl)-benzene (2.5 mM, 1.59 g) was added, and the mixture was stirred at 100 °C for another 10 h. The crude product was obtained when DMSO was removed by vacuum distillation; after purification with methanol, the desired product was obtained as a white powder (1.74 g, 68%).[12] X-ray quality crystals of hpyb were grown by solvothermal synthesis in methanol at 100 °C. ^{1}HNMR (500 MHz; $(CD_3)_2SO$): δ 5.97 (12H, s, CH_2), 8.51 (6H, d, py^6), 7.25 (6H, t, py^5), 7.70 (6H, t, py^4), 7.59 (6H, t, py^3), 7.23 (6H, d, pz^5), 6.66 (6H, d, pz^4). Anal. calcd for $C_{60}H_{48}N_{18}$ (M_r = 1021.14): C, 70.57; H, 4.74; N, 24.69. Found: C, 69.97; H, 4.50; N, 25.53.

Synthesis of $[Ag_2(hpyb)_{0.5}(L1)_{0.5}(NO_3)]\cdot H_2O$ (1). H_2L1 (0.10 mM, 17 mg) was deprotonated in methanol solution using NaOH (0.20 mM, 8 mg). Then hpyb (0.02 mM, 20 mg) and $AgNO_3$ (0.50 mM, 85 mg) were added to the solution. The total volume of the mixture was maintained at 8 mL utilizing methanol as solvent. Then the mixture was sealed in a Teflon-lined stainless steel autoclave reactor (15 mL) and heated at 110 °C for 3 days. After allowing the reaction to cool gradually to room temperature, colorless block crystals of **1** were isolated in 61% yield based on Ag(I). Anal. calcd for $C_{34}H_{28}N_{10}O_6Ag_2$ (M_r = 888.39): C, 45.97; H, 3.18; N, 15.77. Found: C, 45.89; H, 3.12; N, 15.83. IR data (KBr, cm^{-1}): 3735(w), 3394(w), 3100(w), 1748(w), 1599(m), 1523(w), 1497(m), 1434(m), 1366(s), 1231(m), 1156(m), 1096(m), 1060(m), 1000(m), 957(w), 830(w), 776(m), 687(w), 630(w), 518(w).

Synthesis of $[Ag_4(hpyb)(HL2)(NO_3)_2]\cdot 2H_2O$ (2). Compound **2** was made by following the same procedure as that for **1** except that H_3L2 (0.10 mM, 21 mg) was used instead of H_2L1. Colorless block crystals of **2** were separated in 46% yield based on Ag(I). Anal. calcd for $C_{69}H_{56}N_{20}O_{14}Ag_4$ (M_r = 1820.78): C, 45.52; H, 3.10; N, 15.39. Found: C, 46.43; H, 3.21; N, 15.49. IR data (KBr, cm^{-1}): 3835(w), 3739(w), 3433(w), 3088(w), 1716(w), 1594(m), 1506(w), 1367(s), 1279(m), 1227(m), 1098(w), 1003(w), 756(m), 692(w), 431(w).

Synthesis of $[Ag_3(hpyb)_{0.5}(L3)(NO_3)]$ (3). The preparation of compound **3** was similar to that of compound **1** except that H_2L1 was replaced by H_2L3 (0.20 mM, 23.2 mg) and the weight of NaOH was changed to 16.0 mg (0.40 mM). Colorless block crystals of **3** were obtained in 58% yield based on Ag(I). Anal. calcd for $C_{34}H_{26}N_{10}O_7Ag_3$ (M_r = 1010.24): C, 40.42; H, 2.59; N, 13.86. Found: C, 40.33; H, 2.71; N, 13.74. IR data (KBr, cm^{-1}): 3419(w), 3104(w), 2982(w), 1633(w), 1572(m), 1557(s), 1430(s), 1355(m), 1305(s), 1232(m), 1157(m), 1063(m), 957(w), 844(m), 780(m), 686(m), 541(m).

Synthesis of $[Ag_6(hpyb)(L4)_2(NO_3)]\cdot NO_3\cdot 2H_2O$ (4). The preparation of compound **4** was similar to that of compound **3** except that H_2L3 was replaced by H_2L4 (0.20 mM, 33 mg). Colorless block crystals of **4** were isolated in 43% yield based on Ag(I). Anal. calcd for $C_{74}H_{58}N_{22}O_{16}Ag_6$ (M_r = 2158.60): C, 41.17; H, 2.71; N, 14.28. Found: C, 40.09; H, 2.73; N, 14.19. IR data (KBr, cm^{-1}):3307(w), 3078(w), 2823(w), 1573(s), 1453(m), 1381(s), 1229(w), 1093(w), 991(w), 826(m), 744(w), 649(w), 528(w), 426(w).

Synthesis of $[Ag_5(hpyb)_{0.5}(L5)_2(NO_3)]\cdot H_2O$ (5). The preparation of compound **5** was similar to that of compound **1** except that H_2L1 was replaced by H_2L5 (0.40 mM, 66 mg) and the weight of NaOH was changed to 32 mg (0.80 mM). Colorless block crystals of **5** were isolated in 36% yield based on Ag(I). Anal. calcd for $C_{46}H_{34}N_{10}O_{12}Ag_5$ (M_r = 1458.16): C, 37.89; H, 2.35; N, 9.61. Found: C, 38.01; H, 2.34; N, 9.59. IR data (KBr, cm^{-1}): 3421(w), 3105(w), 1599(s), 1502(m), 1436(s), 1375(s), 1267(m), 1230(s), 1096(w), 1000(w), 764(m), 688(w), 442(w).

Synthesis of $\{Ag_4(hpyb)[L6(CH_3)_2]_2\}$ (6). The preparation of compound **6** was similar to that of compound **3** except that

H_2L3 was replaced by H_4L6 (0.20 mM, 55 mg). Colorless block crystals of **6** were isolated in 53% yield based on Ag(I). Anal. calcd for $C_{42}H_{32}N_9O_8Ag_2$ (M_r = 1006.50): C, 50.12; H, 3.20; N, 12.52. Found: C, 50.24; H, 3.18; N, 12.43. IR data (KBr, cm^{-1}): 3845(w), 3743(w), 3438(m), 3106(w), 1724(s), 1598(s), 1486(m), 1433(s), 1386(m), 1338(s), 1254(m), 1100(m), 959(w), 845(w), 751(m), 613(w).

Synthesis of {Ag_6(hpyb)($HL7)_2$[L7(CH_3)]} (7). The preparation of compound **7** was similar to that of compound **1** except that H_2L1 was replaced by 1,2,4-benzenetricarboxylic anhydride (0.30 mM, 61 mg), the weight of NaOH was changed to 24 mg (0.60 mM), and the solvent was replaced by water/methanol ($V_{1:7}$). Colorless block crystals of **7** were isolated in 60% yield based on Ag(I). Anal. calcd for $C_{88}H_{62}N_{18}O_{18}Ag_6$ (M_r = 2306.75): C, 45.82; H, 2.71; N, 10.93. Found: C, 45.75; H, 2.61; N, 10.98. IR data (KBr, cm^{-1}): 3379(m), 3118(w), 1684(m), 1556(s), 1492(s), 1436(s), 1360(s), 1226(m), 1163(m), 1061(m), 856(w), 752(m), 688(w), 558(w).

Synthesis of [Ag_3(hpyb)$_{0.5}$(HL8)]·H_2O (8). The preparation of compound **8** was similar to that of **7** except that 1,2,4-benzenetricarboxylic anhydride was replaced by 4,4′-oxydiphthalic anhydride (0.20 mM, 62 mg). Colorless block crystals of **8** were isolated in 54% yield based on Ag(I). Anal. calcd for $C_{46}H_{33}N_9O_{10}Ag_3$ (M_r = 1195.41): C, 46.22; H, 2.78; N, 10.55. Found: C, 46.27; H, 2.82; N, 10.46. IR data (KBr, cm^{-1}): 3113(w), 2899(w), 2811(w), 1684(w), 1557(s), 1432(s), 1353(s), 1304(m), 1260(s), 1228(s), 1153(m), 1065(m), 959(m), 849(m), 758(s), 686(w), 650(w), 606(w), 439(w).

X-ray crystallography

X-ray single-crystal diffraction data for complexes **1–8** were collected on an Oxford Diffraction Gemini R Ultra diffractometer with graphite-monochromated Mo Kα radiation (λ = 0.71073 Å) at 293 K. All the structures were solved by direct methods using the SHELXS program and refined by full-matrix least-squares methods with the SHELXL program, respectively. The Fourier difference maps determined all non-hydrogen atoms of the complexes, which were optimized with anisotropic temperature parameters. The disordered atoms (O3 and C36 in **2**, O7 in **3**, O13, O1W and O2W in **4**, C12 and O9 in **5**, C41, C45, O9 and O10 in **7**, O1W in **8**) were divided over two sites with the total occupancy of 1. The free water molecules in complexes **1**, **2** and **5** couldn't identify hydrogen atoms from suitable residual peaks. The topological research of complex **5** was analyzed by using the OLEX program. The detailed crystallographic data and structure refinement parameters for **1–8** are summarized in Table 1. Selected bond distances and angles for compounds are given in the ESI† (Tables S1–S8).

Results and discussion

Structure of hpyb

The free hpyb ligand crystallizes in the monoclinic space group $P2_1/c$, and its asymmetric unit contains half molecule. The six 3-(2-pyridyl)pyrazole groups of the hpyb ligand take up–down arrangements at intervals as shown in Fig. 1. The flexible methylene spacers allow the six 3-(2-pyridyl)pyrazole groups to rotate, with their coordination sites adopting four inward and two outward fashions.

Structure of [Ag_2(hpyb)$_{0.5}$(L1)$_{0.5}$(NO_3)]·H_2O (1)

The asymmetric unit of compound **1** is formed by two Ag(I) ions, half hpyb ligand, half L1 anion, one nitrate anion and one free water molecule. As shown in Fig. 2a, the coordination environments of Ag1 and Ag2 are entirely different. Ag1 is five-coordinated in a tetragonal pyramid coordination geometry by four N atoms from one hpyb ligand (Ag–N 2.451(5) to 2.554(3) Å) and one O atom from an L1 anion (Ag–O 2.274(4) Å). Ag2 is three-coordinated in a T-shaped coordination geometry by two N atoms from one hpyb ligand (Ag–N 2.347(3) and 2.348(5) Å) and one O atom from an L1 anion (Ag–O 2.151(5) Å). Each hpyb ligand links with four Ag(I) ions, with its six 3-(2-pyridyl)pyrazole groups displaying a 1,2,3-up/4,5,6-down fashion. The L1 anion lies at an inversion center, which supported Ag1 and Ag2 ions to form a binuclear unit with the hpyb ligand. The distance of Ag1···Ag2 is 3.055(3) Å, smaller than twice the van der Waals radius for silver atoms (3.44 Å), indicating the existence of a Ag···Ag interaction (Fig. S1†). The binuclear Ag(I) units are generated by L1 anions to constitute a 1D chain (Fig. 2b). The chains are further extended *via* intermolecular π–π stackings between the pyrazole and pyridine rings of the hpyb ligands (centroid-to-centroid distance: 3.940 Å) to yield a 2D supramolecular layer (Fig. 2c). The layers are linked by another double π–π interactions between the pyrazole and pyridine rings of the hpyb ligands (centroid-to-centroid distances: 3.645 Å and 3.610 Å, respectively) to form a 3D supramolecular architecture (Fig. 2d).

Structure of [Ag_4(hpyb)(HL2)($NO_3)_2$]·$2H_2O$ (2)

When the ligand H_2L1 in compound **1** was replaced by H_3L2, a similar structure of **2** was obtained. The spatial configurations of Ag1 and Ag2 in **2** are identical to those of **1** (Fig. 3a). An HL2 anion is located at an inversion center, and its protonated middle carboxyl group is kept uncoordinated. Ag1 and Ag2 ions are gathered by the HL2 anion and the hpyb ligand together to form a binuclear unit, with the distance of 2.926(7) Å (Fig. S2†). The HL2 anion bridges the binuclear Ag(I) units to form a 1D chain along the *c*-axis (Fig. 3b). The chains are sequentially joined by π–π interactions (centroid-to-centroid distance: 3.789 Å) to generate a 3D supramolecular architecture (Fig. 3c).

Structure of [Ag_3(hpyb)$_{0.5}$(L3)(NO_3)] (3)

The asymmetric unit of compound **3** contains three Ag(I) ions, half hpyb ligand, one L3 anion and one nitrate anion. As shown in Fig. 4a, Ag1 is five-coordinated by two N atoms from one hpyb ligand and three O atoms from two L3 anions

Table 1 Crystal data and structure refinements for compounds **1**–**8**

	1	**2**	**3**	**4**	**5**	**6**	**7**	**8**
Formula	$C_{34}H_{28}N_{10}O_6Ag_2$	$C_{69}H_{56}N_{20}O_{14}Ag_4$	$C_{34}H_{26}N_{10}O_7Ag_3$	$C_{74}H_{58}N_{22}O_{16}Ag_6$	$C_{46}H_{34}N_{10}O_{12}Ag_5$	$C_{42}H_{32}N_9O_8Ag_2$	$C_{88}H_{62}N_{18}O_{18}Ag_6$	$C_{46}H_{33}N_9O_{10}Ag_3$
Fw	888.40	1820.82	1010.26	2158.64	1458.18	1006.51	2306.78	1195.42
Space group	$P\bar{1}$	$C2/c$	$P\bar{1}$	$P\bar{1}$	$P\bar{1}$	$P\bar{1}$	$P\bar{1}$	$P\bar{1}$
a (Å)	11.6530(6)	20.6570(8)	10.9860(4)	13.0400(8)	12.6750(5)	11.4860(6)	10.3250(7)	11.927(5)
b (Å)	12.1570(7)	14.2360(6)	12.3070(5)	13.9500(11)	14.3120(7)	12.9510(8)	14.1580(10)	13.940(5)
c (Å)	13.8700(8)	23.3580(9)	13.8910(6)	22.5400(15)	15.2200(7)	13.9760(6)	14.9160(10)	14.060(5)
α (deg.)	67.552(5)	90	82.446(4)	107.566(7)	106.736(4)	85.015(4)	68.417(7)	71.773(5)
β (deg.)	89.980(6)	103.847(4)	68.707(4)	96.682(5)	99.655(4)	79.768(4)	71.336(7)	79.535(5)
γ (deg.)	69.718(5)	90	71.970(3)	96.412(6)	115.188(4)	65.610(5)	81.650(6)	74.679(5)
V (Å^3)	1683.55(16)	6669.3(5)	1663.60(12)	3835.5(5)	2254.41(18)	1863.14(17)	1920.0(2)	2128.9(14)
Z	2	4	2	2	2	2	1	2
D_{calcd} (g cm^{-3})	1.753	1.813	2.017	1.869	2.148	1.794	1.995	1.865
F(000)	888	3620	994	2132	1422	1010	1142	1186
Observed reflection/unique	12 008/7666	14 160/7698	11 955/7492	24 313/13 752	16 828/10 342	14 064/8471	13 377/8725	13 275/7474
R(int)	0.0167	0.0276	0.0222	0.0697	0.0297	0.0351	0.0266	0.0466
GOF on F^2	1.032	1.010	1.022	0.988	1.015	1.021	1.067	1.023
$R_1{}^a$ $[I > 2\sigma(I)]$	0.0486	0.0571	0.0435	0.0841	0.0498	0.0612	0.0512	0.0646
w$R_2{}^b$	0.1468	0.1736	0.1032	0.2334	0.1245	0.1630	0.1197	0.1761

[a] $R_1 = \sum||F_o| - |F_c||/\sum|F_o|$. [b] $wR_2 = |\sum w(|F_o|^2 - |F_c|^2)|/\sum|w(F_o{}^2)^2|^{1/2}$.

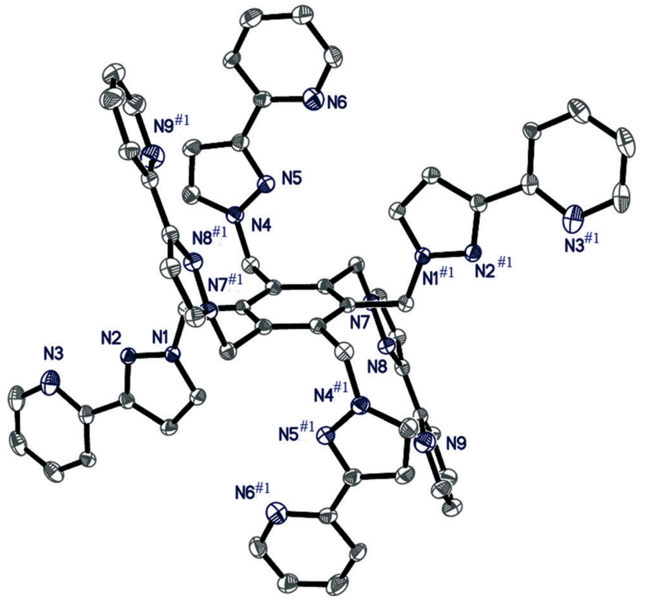

Fig. 1 ORTEP diagram of a hpyb ligand.

in a distorted tetragonal pyramid geometry. Ag2 is three-coordinated in a T-shaped geometry by two N atoms from one hpyb ligand and one O atom from an L3 anion. Ag3 is four-coordinated by two N atoms from one hpyb ligand and two O atoms from L3 and nitrate anions in a distorted tetrahedral geometry. Each hpyb ligand coordinates with six Ag(I) ions. The Ag(I) ions are linked to each other by an L3 anion and a hpyb ligand to yield a trinuclear Ag(I) cluster, with Ag⋯Ag distances of 2.981 and 3.461 Å (Fig. S3†). These Ag(I) clusters are linked by L3 anions to form a chain (Fig. 4b), which are further constructed by π–π interactions between the pyrazole and pyridine rings (centroid-to-centroid distance: 3.645 Å) to form a supramolecular layer (Fig. 4c).

Structure of $[Ag_6(hpyb)(L4)_2(NO_3)]\cdot NO_3\cdot 2H_2O$ (4)

The asymmetric unit of compound 4 is composed of six Ag(I) ions, one hpyb ligand, two L4 anions, two nitrate anions and two free water molecules. Ag1–Ag3 display distorted tetrahedral geometries, in which Ag1 is coordinated by one hpyb ligand and one L4 anion in a $[AgN_3O]$ fashion, Ag2 is surrounded by one hpyb and one L4 anion in a $[AgN_3O]$ fashion, while Ag3 is environed by one hpyb ligand and two L4 anions in a $[AgNO_3]$ mode. Ag4 and Ag6 are five-coordinated in anomalistic tetragonal pyramid coordination geometries, in which Ag4 is surrounded by one hpyb ligand, one L4 anion and one nitrate anion in a $[AgN_3O_2]$ fashion and Ag6 is coordinated by one hpyb and two L4 anions in a $[AgN_2O_3]$ fashion. Ag5 is three-coordinated in a T-shaped geometry by the hpyb ligand and the L4 anion in a $[AgN_2O]$ mode. Each hypb coordinates to six Ag(I) ions. Two binuclear Ag(I) units are formed by the hpyb ligand and two kinds of L4 anions together (with Ag2⋯Ag3 and Ag5⋯Ag6 distances of 3.027 and 3.053 Å, Fig. S4†). Each L4 anion coordinates to four Ag(I) ions, which connects the Ag(I) ions and hpyb ligands to

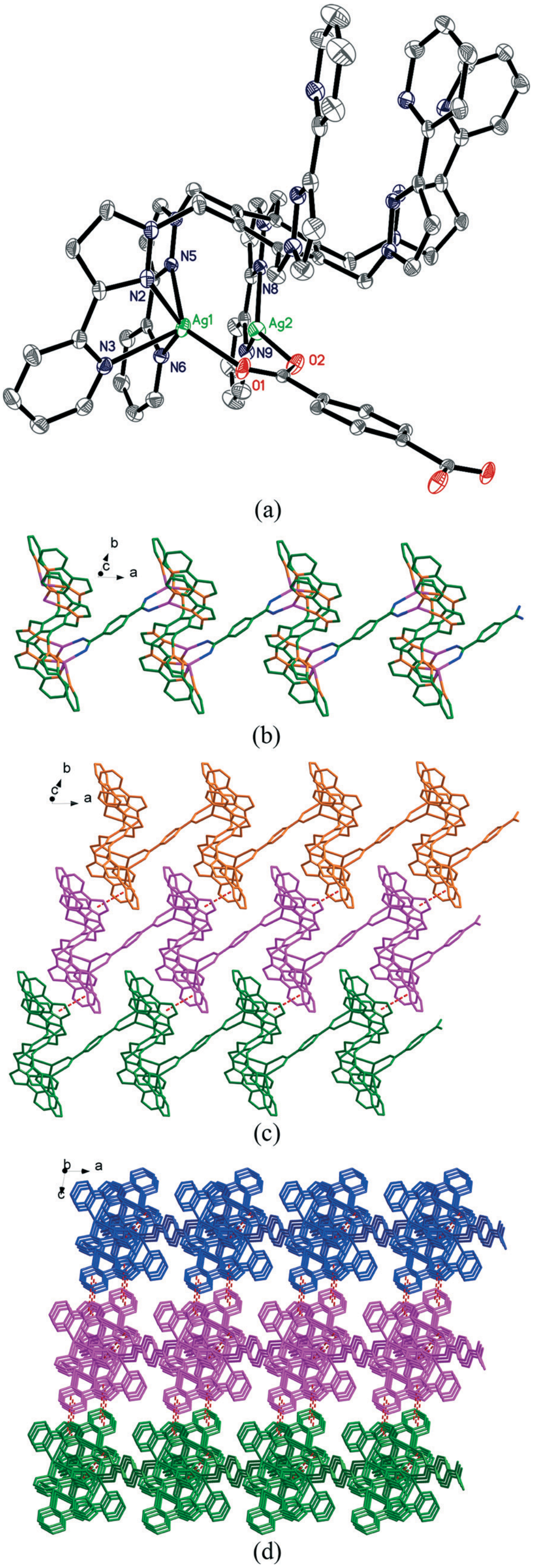

Fig. 2 (a) Coordination environments of the Ag(I) cations in **1**. (b) View of the 1D chain. (c) View of the 2D supramolecular layer formed *via* π–π interactions. (d) View of the 3D supramolecular architecture formed by π–π interactions.

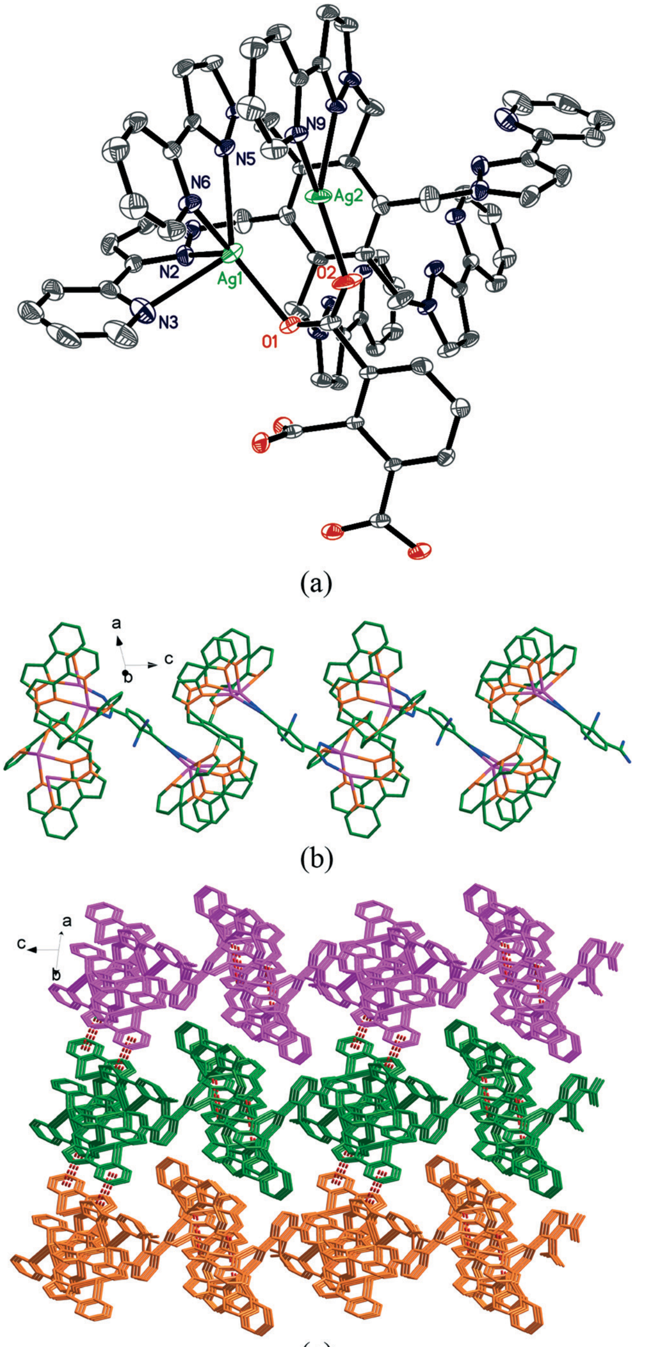

Fig. 3 (a) Coordination environments of the Ag(I) cations in **2**. (b) View of the 1D chain. (c) View of the 3D supramolecular architecture formed by π–π interactions.

form a 1D chain (Fig. 5b). Due to the double π–π interactions between the pyrazole rings and pyridine rings of the hpyb ligands (centroid-to-centroid distances: 3.937 Å and 3.588 Å, respectively), the chains are linked into a 2D supramolecular layer. These layers are further connected by another type of π–π interactions between the pyridine rings of the hpyb ligands (centroid-to-centroid distance: 3.720 Å) to generate the final 3D supramolecular architecture.

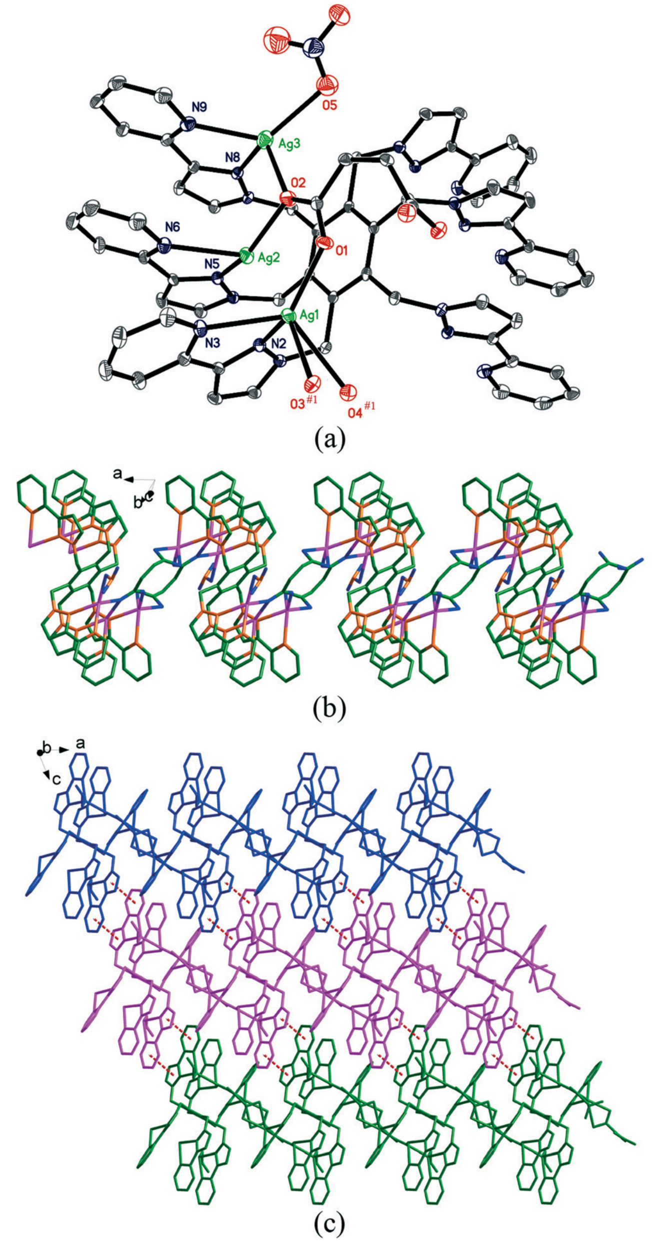

Fig. 4 (a) Coordination environments of the Ag(I) cations in **3**. (b) View of the 1D chain. (c) View of the 2D supramolecular layer formed *via* π–π interactions.

Structure of $[Ag_5(hpyb)_{0.5}(L5)_2(NO_3)]\cdot H_2O$ (5)

When H_2L5 was introduced to this system, a novel 3D framework of **5** was obtained. Single-crystal X-ray analysis indicates that the asymmetric unit of **5** contains five Ag(I) ions, half hpyb ligand, two L5 anions, one nitrate anion and one free water molecule. As shown in Fig. 6a, Ag1 is three-coordinated in a T-shaped coordination geometry by two N atoms from one hpyb ligand and one O atom from an L5 anion. The other Ag(I) ions are four-coordinated, displaying distorted tetrahedral geometries with distinct coordination environments. In which Ag2 bonds to two N atoms from one hpyb ligand and two O atoms from different L5 anions, Ag3 and Ag4 are both surrounded by four O atoms from L5 anions and nitrate ions, while Ag5 connects one N atom from the hpyb ligand and three O atoms from two L5 and one nitrate anions. Significantly, there exist two kinds of Ag···Ag interactions supported by the hpyb ligand and L5 anions, in which Ag1, Ag2 and Ag3 are gathered to a hexanuclear cluster, while Ag4 and Ag5 are connected into a tetranuclear cluster (Fig. S5a†). These two types of clusters are interlinked by the hpyb ligands and L5 anions to form a 2D layer. The nitrate anions further connect the layers into a 3D framework (Fig. 6b).

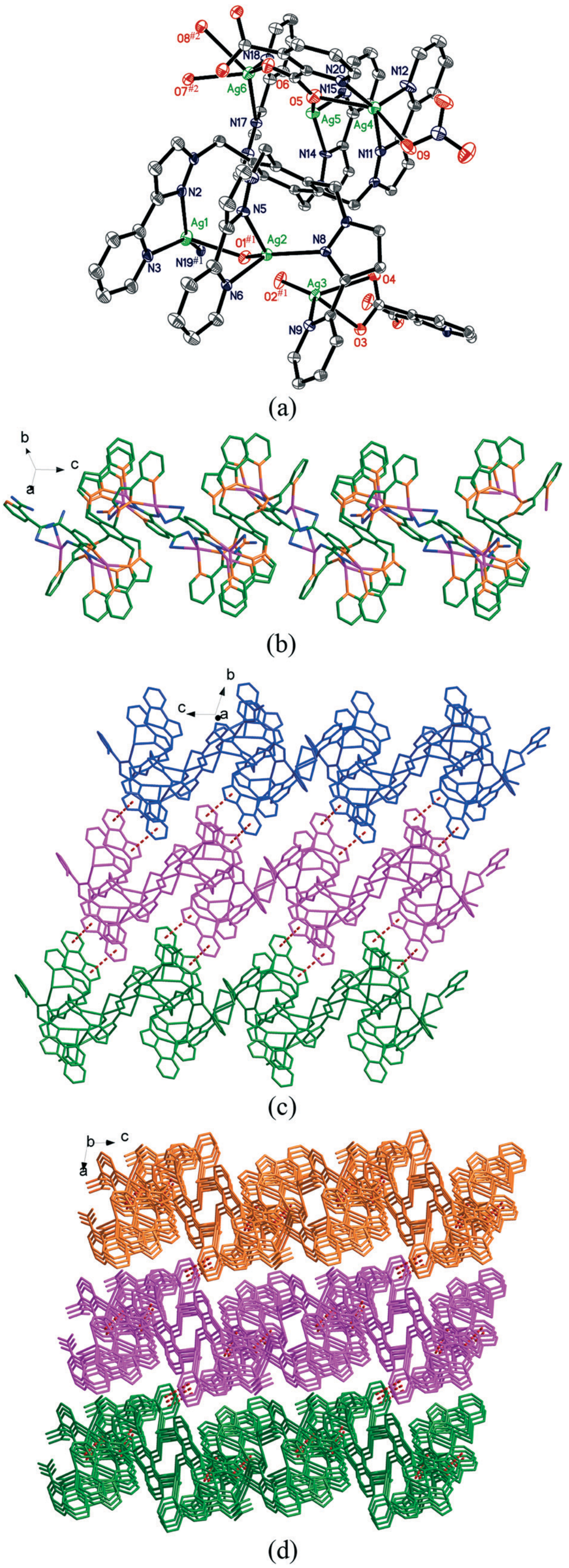

(a)

(b)

(c)

(d)

Fig. 5 (a) Coordination environments of the Ag(I) cations in **4**. (b) View of the 1D chain. (c) View of the 2D supramolecular layer formed *via* π–π interactions. (d) View of the 3D supramolecular architecture formed by π–π interactions.

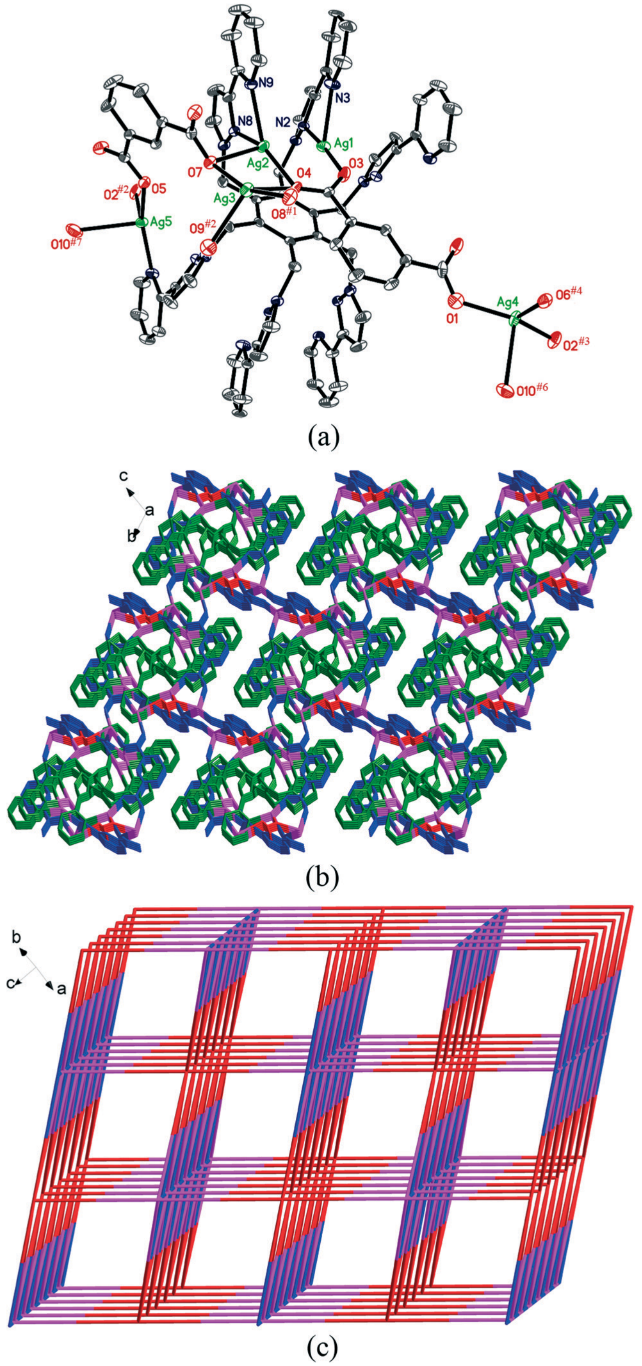

(a)

(b)

(c)

Fig. 6 (a) Coordination environments of the Ag(I) cations in **5**. (b) View of the 3D framework. (c) View of the 3D trinodal (4,8)-connected net.

From a topological perspective, compound **5** is a 3D trinodal (4,8)-connected net with a $(3^4{\cdot}4^2)(3^4{\cdot}4^{12}{\cdot}5^8{\cdot}6^4)_2$ topology (Fig. 6c), where the hpyb ligands, the tetranuclear clusters and the hexanuclear clusters are defined as 4-, 8- and 8-connected nodes, respectively (Fig. S5b†).

Structure of $\{Ag_4(hpyb)[L6(CH_3)_2]_2\}$ (6)

When H_4L6 was introduced into the reaction system, an esterified anion $L6(CH_3)_2$ appeared. The asymmetric unit of compound **6** contains two Ag(I) ions, half hpyb ligand and one $L6(CH_3)_2$ anion. As illustrated in Fig. 7a, Ag1 is four-coordinated by two N atoms from the hpyb ligand and two O atoms from two $L6(CH_3)_2$ anions in a distorted tetrahedral geometry. Ag2 displays a T-shaped coordination geometry by two N atoms from one hpyb ligand and one O atom from an $L6(CH_3)_2$ anion. Unlike the hpyb in previous compounds, only four 3-(2-pyridyl)pyrazole arms of the hpyb ligand in **6** coordinate with Ag(I) cations, while the other two arms are kept free. Ag1 and Ag2 are assembled into a binuclear Ag(I) unit by the hpyb ligand and the carboxylate group of $L6(CH_3)_2$ anion together (Fig. S6†). The adjacent binuclear units are further linked by $L6(CH_3)_2$ anions in different directions to form a 2D sheet (Fig. 7b). Two types of π–π interactions between the hpyb ligands (centroid-to-centroid distances: 3.657 and 3.900 Å) integrate these sheets to form a 3D supramolecular architecture (Fig. 7c).

Structure of $\{Ag_6(hpyb)(HL7)_2[L7(CH_3)]\}$ (7)

Somewhat similar to compound **6**, the H_3L7 is partially esterified by methanol to form $L7(CH_3)$ anions. So the asymmetric unit of compound **7** contains three Ag(I) ions, half hpyb ligand, one HL7 anion and half $L7(CH_3)$ anion. As shown in Fig. 8a, Ag1 is five-coordinated by two N atoms from one hpyb ligand and three O atoms from two HL7 anions in a distorted tetragonal pyramid geometry. Ag2 and Ag3 are both three-coordinated, displaying T-shaped $[AgN_2O]$ coordination geometries, in which Ag2 connects by one hpyb and one HL7 anion and Ag3 links to one hpyb ligand and one $L7(CH_3)$ anion. A trinuclear cluster is formed by Ag1, Ag2 and Ag3 ions. Unlike previous compounds, the trinuclear Ag(I) cluster in compound **7** is supported by the hpyb ligand only without any organic anions (Fig. S7a†). Each of the HL7 and $L7(CH_3)$ anions links with two Ag(I) ions. In this fashion, the trinuclear Ag(I) clusters are interlinked through organic ligands to afford a wave-like layer (Fig. S7b†). The layers are further stabilized by π–π interactions (centroid-to-centroid distance: 3.984 Å) between the benzene rings of HL7 and $L7(CH_3)$ anions (Fig. 8b).

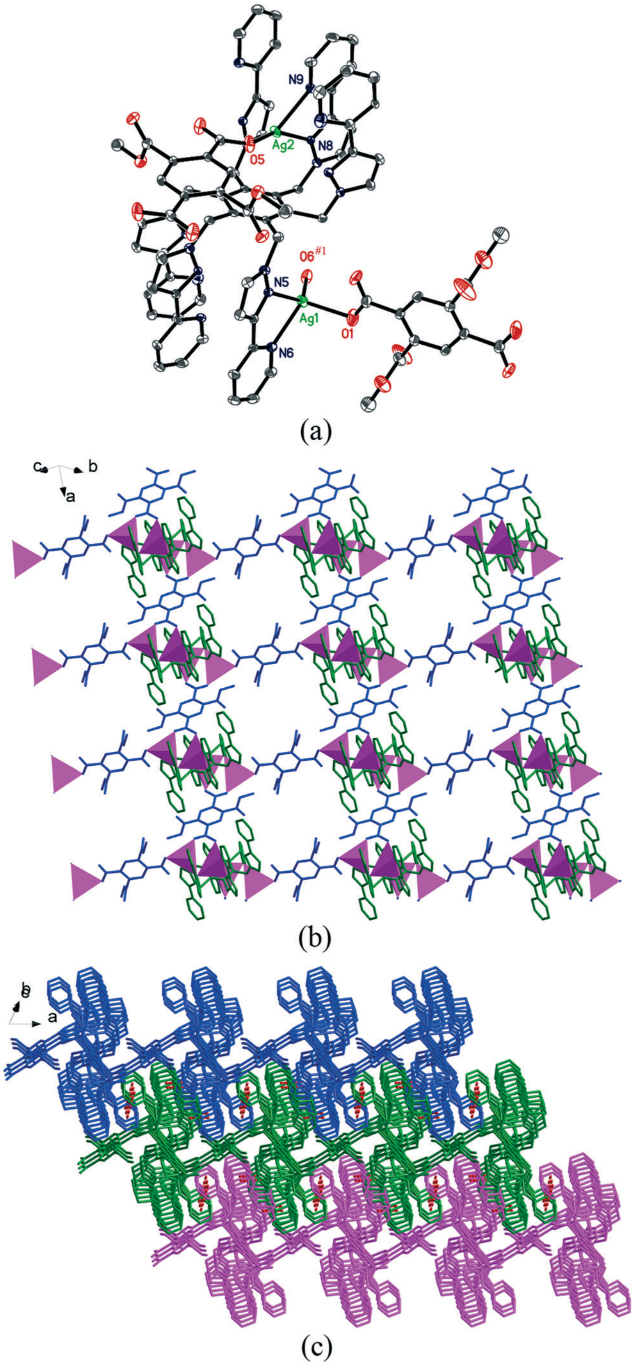

Fig. 7 (a) Coordination environments of the Ag(I) cations in **6**. (b) View of the 2D sheet. (c) View of the 3D supramolecular architecture formed by π–π interactions.

Structure of $[Ag_3(hpyb)_{0.5}(HL8)]{\cdot}H_2O$ (8)

H_4L8 is a relatively flexible ligand because of its rotatable ether bond. This flexibility affords it the potential to construct a more extensive Ag(I) cluster and to sustain a novel network. The asymmetric unit of compound **8** contains three Ag(I) ions, half hpyb ligand, one HL8 anion and one free water molecule. As depicted in Fig. 9a, Ag1 and Ag3 are both four-coordinated, displaying distorted $[AgN_2O_2]$ tetrahedral geometries, in which Ag1 coordinates to one hpyb ligand and two HL8 anions, while Ag3 connects with one hpyb ligand and one HL8 anion. Ag2 is five-coordinated in a distorted $[AgN_2O_3]$ tetragonal pyramid geometry by one hpyb ligand

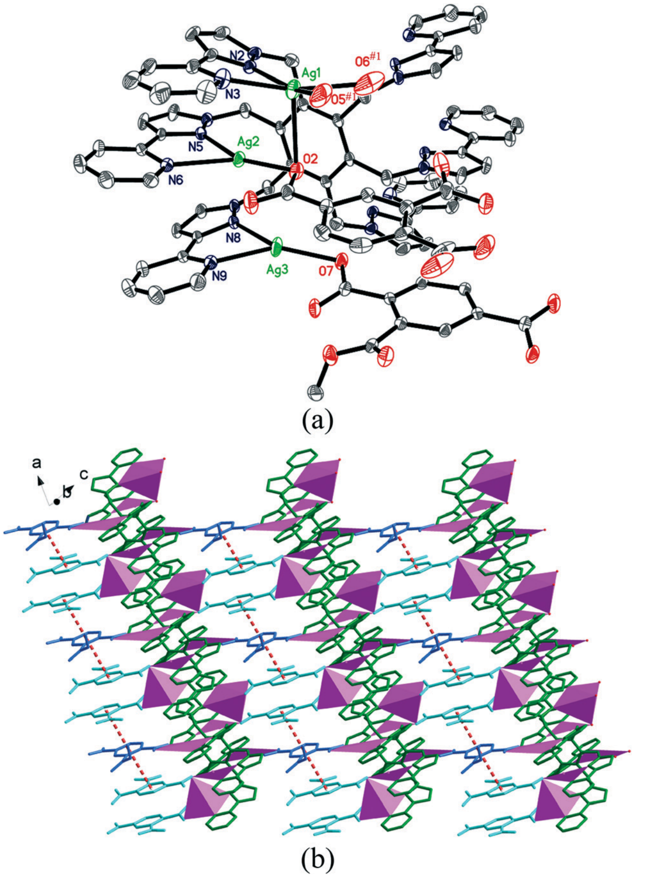

Fig. 8 (a) Coordination environments of the Ag(I) cations in **7**. (b) View of the 2D layer of **7**.

and two HL8 anions. Each HL8 anion links to five Ag(I) ions. In this manner, a hexanuclear Ag(I) cluster is formed by HL8 anions and hpyb ligands together (Fig. S8†). These clusters are connected by HL8 anions to generate a 2D layer (Fig. 9b). The existence of π–π interactions (centroid-to-centroid distance: 3.925 Å) between the pyrazole rings and pyridine rings further extend the layers into a 3D supramolecular architecture (Fig. 9c).

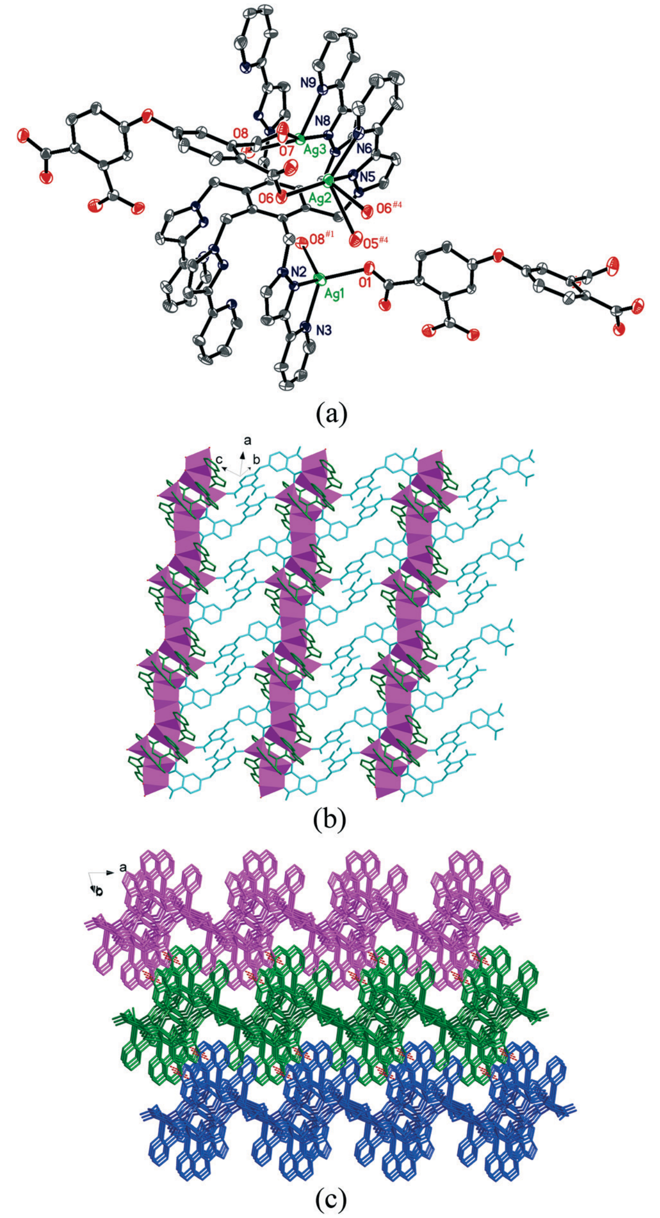

Fig. 9 (a) Coordination environments of the Ag(I) cations in **8**. (b) View of the 2D network. (c) View of the 3D supramolecular architecture formed by π–π interactions.

Influence of polycarboxylate anions

Compounds **1–8** were synthesized under similar conditions with an unchanging N-donor ligand and an inorganic salt. Their diverse structures are primarily ascribed to the difference in polycarboxylic acids. In this series, polycarboxylic anions have different spacers, flexibilities and number of carboxylate groups. These factors can influence the motifs of the complexes. Compounds **1** and **5** exhibit the effects of carboxylate positions on their structures. Although both L1 and L5 act as dicarboxylate anions with benzene rings, the positions of the carboxylate groups are different (*p*-phenyl and *m*-phenyl). Different lengths of spacers influence the numbers of the coordinated Ag(I) ions. As a result, Ag(I) ions are bridged by polycarboxylic anions to form binuclear units in **1** and tetranuclear and hexanuclear clusters in **5**, respectively. This difference is magnified further by the extension of the final structures, where **1** shows a 1D chain, but **5** displays a 3D framework. Generally, increasing the number of carboxylate groups can result in a higher dimensionality of the structures.[13] However, the coordination modes of the polycarboxylates play more important roles in the final structures of complexes **2** and **6–8**. The tri- and tetra-basic carboxylic acids H_3L2 and H_4L8 in **2** and **8** are partly deprotonated to HL2 and HL8, respectively. The H_4L6 and H_3L7 in **6** and **7** are esterified by methanol molecules to form $L6(CH_3)_2$ and $L7(CH_3)$ anions, respectively. As a result, instead of the 3D expanded framework, these compounds only display 1D chain or 2D layers.

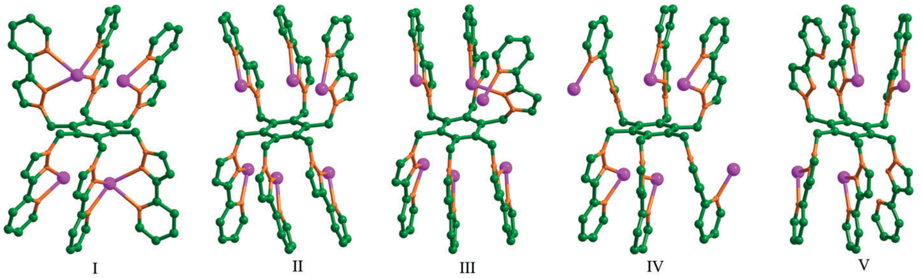

Chart 2 The coordination modes of hpyb in **1**–**8**.

Coordination modes of the hpyb ligand

In this work, the hpyb ligand exhibits five types of coordination patterns during the self-assembly process (Chart 2). Different from the 1,3,5-above/2,4,6-below fashion of the free hpyb ligand, these five patterns all show a 1,2,3-above/4,5,6-below fashion. The change of the fashion indicates that the coordinated Ag(I) ions influence the configuration of the hpyb ligand. The hpyb ligand in these compounds can connect four or six Ag(I) ions. Different coordination numbers of the ligand lead to the distinction of the Ag···Ag subunits. Each hpyb in compounds **1** (pattern I), **2** (pattern I) and **6** (pattern V) links with four Ag(I) ions using its six 3-(2-pyridyl)pyrazole arms chelating to Ag(I) ions or is kept free. Binuclear Ag(I) units were formed in these compounds. When a highly connected hpyb ligand (connected to six Ag ions) appeared in structures **3** (pattern II), **5** (pattern IV), **7** (pattern II) and **8** (pattern II), tri-, tetra- or hexanuclear Ag(I) clusters were generated. The hpyb ligand in compound **4** also links six metal ions (in pattern III), and the generation of the binuclear Ag(I) units may be attributed to the synergistic coordination effect of the 2,3-pyridinedicarboxylate (L4) anion.

PXRD results

The experimental and computer-simulated PXRD patterns of compounds **1**–**8** are shown in Fig. S9,† which demonstrate that the synthesized bulk materials and the measured single crystals are the same.

Luminescence properties

The solid-state emission spectra of the hpyb ligand and compounds **1**–**8** were measured at ambient temperature (Fig. 10). As a highly conjugated ligand, hpyb exhibits a strong emission band with a maximum at 529 nm upon excitation at 343 nm. The emission can be attributed to the π* → π or π* → n transitions.[14] Compounds **1**–**8** exhibit the emission maximum at 514, 590, 546, 522, 516, 572, 524 and 588 nm upon excitation at 370 nm at room temperature, respectively. Obviously, the peak positions of compounds **1**–**8** are somewhat similar to those of the free hpyb ligand. This result indicates that the emissions of **1**–**8** mainly originate from ligand-based luminescence.[15] Compared with the emission of the free hpyb, compounds **2**, **3**, **6** and **8** exhibit obviously red shifts. Based on the previous literature, red shifts might be attributed to the different architectures featuring different intensities of supramolecular interactions (such as Ag···Ag and π–π interactions).[16] The different emission peaks of compounds **1**–**8** may also be influenced by polycarboxylate anions.[17] Compared with hpyb, although free polycarboxylic acids show relatively lower emissions due to the effects of their electron-withdrawing carboxylate groups,[18] they may also make contributions to the emissions, because the coordination of polycarboxylates to Ag(I) ions may increase the conformational rigidity of organic anions and reduce the nonradiative decay of their excited state.[17]

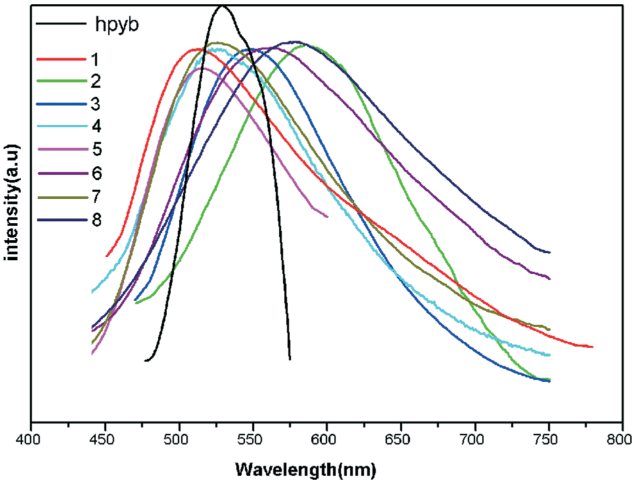

Fig. 10 Emission spectra of the hpyb ligand and compounds **1**–**8** in the solid state at room temperature.

Conclusion

Eight coordination polymers formed by a N-donor hpyb ligand have been synthesized by a solvothermal method. This series of compounds exhibits diverse 1D, 2D and 3D structural motifs based on the variable hpyb ligand and the choice of polycarboxylic acids. Numerous Ag···Ag and π–π interactions become the most exciting features of these complexes. It is noteworthy that such a N-donor ligand with such coordination patterns and the special metal···metal interactions are rare in the past reports. Moreover, all of these complexes exhibit broad visible light emission bands at room temperature, which suggests that they may be good candidates for optical materials.

Acknowledgements

This work was supported by the National Natural Science Foundation of China (grant no. 21071028, 21001023, 21277022, 21371030, and 21301026) and the Fundamental Research Funds for the Central Universities of China.

References

1 (*a*) A. Castiñeiras and R. Pedrido, *Inorg. Chem.*, 2008, **47**, 5534; (*b*) J. Y. Liu, Z. Y. Liu, L. J. Zhang, Y. Y. Wang, P. Yang, Y. Wang, B. Ding and X. J. Zhao, *CrystEngComm*, 2013, **15**, 6413; (*c*) C. Yang, O. Elbjeirami, C. S. P. Gamage, H. V. R. Dias and M. A. Omary, *Chem. Commun.*, 2011, **47**, 7434; (*d*) F. F. Li, J. F. Ma, S. Y. Song, J. Yang, H. Q. Jia and N. H. Hu, *Cryst. Growth Des.*, 2006, **6**, 209.

2 (*a*) N. C. Kasuga, R. Yoshikawa, Y. Sakai and K. Nomiya, *Inorg. Chem.*, 2012, **51**, 1640; (*b*) S. D. Bian, J. H. Jia and Q. M. Wang, *J. Am. Chem. Soc.*, 2009, **131**, 3422; (*c*) J. C. Jin, Y. Y. Wang, W. H. Zhang, A. S. Lermontov, E. K. Lermontova and Q. Z. Shi, *Dalton Trans.*, 2009, 10181.

3 (*a*) J. Hunger, H. Krautscheid and J. Sieler, *Cryst. Growth Des.*, 2009, **9**, 4613; (*b*) A. Karmakar and I. Goldberg, *CrystEngComm*, 2011, **13**, 350.

4 (*a*) Y. Zhao, P. Zhang, B. Li, X. G. Meng and T. L. Zhang, *Inorg. Chem.*, 2011, **50**, 9097; (*b*) K. Nomiya, S. Takahashi, R. Noguchi, S. Nemoto, T. Takayama and M. Oda, *Inorg. Chem.*, 2000, **39**, 3301; (*c*) P. R. Wei, T. C. W. Mac and D. A. Atwood, *Inorg. Chem.*, 1998, **37**, 2605.

5 (*a*) K. P. Rao, M. Higuchi, J. Duan and S. Kitagawa, *Cryst. Growth Des.*, 2013, **13**, 981; (*b*) G. Z. Liu, X. D. Li, X. L. Li and L. Y. Wang, *CrystEngComm*, 2013, **15**, 2428; (*c*) W. Wang, W. Q. Kan, J. Yang and J. F. Ma, *CrystEngComm*, 2013, **15**, 3824.

6 (*a*) X. Feng, L. Liu, L. Y. Wang, H. L. Song, Z. Q. Shi, X. H. Wu and S. W. Ng, *J. Solid State Chem.*, 2013, **206**, 277; (*b*) H. Wu, J. Yang, Z. M. Su, S. R. Batten and J. F. Ma, *J. Am. Chem. Soc.*, 2011, **133**, 11406.

7 C. Femoni, S. Muzzioli, A. Palazzi, S. Stagni, S. Zacchini, F. Monti, G. Accorsi, M. Bolognesi, N. Armaroli, M. Massi, G. Valenti and M. Marcaccio, *Dalton Trans.*, 2012, **10**, 1039.

8 D. A. McMorran and P. J. Steel, *Inorg. Chem. Commun.*, 2003, **6**, 43.

9 (*a*) J. Yang, J. F. Ma, Y. Y. Liu, J. C. Ma and S. R. Batten, *Inorg. Chem.*, 2007, **46**, 6542; (*b*) Y. C. He, J. Yang, G. C. Yang, W. Q. Kan and J. F. Ma, *Chem. Commun.*, 2012, **48**, 7859; (*c*) S. Y. Song, X. Z. Song, S. N. Zhao, C. Qin, S. Q. Su, M. Zhu, Z. M. Hao and H. J. Zhang, *Dalton Trans.*, 2012, **41**, 10412.

10 (*a*) S. P. Argent, H. Adams, T. Riis-Johannessen, J. C. Jeffery, L. P. Harding and M. D. Ward, *J. Am. Chem. Soc.*, 2006, **128**, 72; (*b*) A. Stephenson, S. P. Argent, T. Riis-Johannessen, I. S. Tidmarsh and M. D. Ward, *J. Am. Chem. Soc.*, 2011, **133**, 858; (*c*) N. K. Al-Rasbi, I. S. Tidmarsh, S. P. Argent, H. Adams, L. P. Harding and M. D. Ward, *J. Am. Chem. Soc.*, 2008, **130**, 11641; (*d*) R. Q. Zou, X. H. Bu and R. H. Zhang, *Inorg. Chem.*, 2004, **43**, 5382; (*e*) T. L. Hu, J. R. Li, C. S. Liu, X. S. Shi, J. N. Zhou, X. H. Bu and J. Ribas, *Inorg. Chem.*, 2006, **45**, 162; (*f*) R. Q. Zou, C. S. Liu, Z. Huang, T. L. Hu and X. H. Bu, *Cryst. Growth Des.*, 2006, **6**, 99; (*g*) T. L. Hu, R. Q. Zou, J. R. Li and X. H. Bu, *Dalton Trans.*, 2008, 1302.

11 (*a*) H. Brunner and T. Scheck, *Chem. Ber.*, 1992, **125**, 701; (*b*) Y. Lin and S. A. Lang, *J. Heterocycl. Chem.*, 1977, **14**, 345; (*c*) A. D. U. Hardy, D. D. MacNicol and D. R. Wilson, *J. Chem. Soc., Perkin Trans. 2*, 1979, 1011.

12 Z. Zhang, J. F. Ma, Y. Y. Liu, W. Q. Kan and J. Yang, *CrystEngComm*, 2013, **15**, 2009.

13 H. Y. Liu, J. F. Ma, Y. Y. Liu and J. Yang, *CrystEngComm*, 2013, **15**, 2699.

14 J. H. Yang, S. L. Zheng, X. L. Yu and X. M. Chen, *Cryst. Growth Des.*, 2004, **4**, 831.

15 J. F. Ma, J. Yang, S. L. Li and S. Y. Song, *Cryst. Growth Des.*, 2005, **5**, 807.

16 (*a*) Y. B. Dong, H. X. Xu, J. P. Ma and R. Q. Huang, *Inorg. Chem.*, 2006, **45**, 3325; (*b*) J. H. Yang, S. L. Zheng, X. L. Yu and X. M. Chen, *Cryst. Growth Des.*, 2004, **4**, 831; (*c*) K. J. Wei, Y. S. Xie, J. Ni, M. Zhang and Q. L. Liu, *Inorg. Chem. Commun.*, 2006, **9**, 926.

17 (*a*) H. Y. Liu, H. Wu, J. F. Ma, J. Yang and Y. Y. Liu, *Dalton Trans.*, 2009, 7957; (*b*) Y.-Y. Liu, J.-C. Ma, L.-P. Zhang and J.-F. Ma, *J. Coord. Chem.*, 2008, **61**, 3583.

18 Z. Zhang, J.-F. Ma, Y.-Y. Liu, W.-Q. Kan and J. Yang, *Cryst. Growth Des.*, 2013, **13**, 4338.